Modulation of autoimmune arthritis severity in mice by Apolipoprotein E (ApoE) and cholesterol.

Short title: ApoE and cholesterol in inflammation

Pilar Alvarez[1], Fernanda Genre[2], Marcos Iglesias[2], Juan Jesús Augustin[1,2], Esther Tamayo[2], Joan Carles Escolà-Gil[3], Bernardo Lavín[4], Francisco Blanco-Vaca[3], Ramón Merino[1,2] and Jesús Merino[2].

[1]Instituto de Biomedicina y Biotecnología de Cantabria, Consejo Superior de Investigaciones Científicas-Universidad de Cantabria-SODERCAN, Santander, Spain, [2]Departamento de Biología Molecular-IDIVAL Universidad de Cantabria, Santander, Spain and [3]Institut d'Investigacions Biomèdiques (IIB) Sant Pau, Barcelona, Spain; Departament de Bioquímica i Biologia Molecular, Universitat Autònoma de Barcelona, Barcelona; CIBER de Diabetes y Enfermedades Metabólicas Asociadas, Barcelona Spain. [4]Servicio de Análisis Clínicos, Hospital Universitario Marqués de Valdecilla, Santander, Spain.

Correspondence: Dr. Jesús Merino, Departamento de Biología Molecular, Facultad de Medicina, Cardenal Herrera Oria s/n, 39011 Santander, Spain.

Phone: 34 942 201956; Fax: 34 942 201945; e-mail: merinoj@unican.es

KEYWORDS: ApoE, hypercholesterolemia, collagen type II-induced arthritis, LDLR

LIST OF ABBREVIATIONS

ApoE: apolipoprotein E

TC: total cholesterol

LDL: low-density lipoprotein

oxLDL: oxidized LDL

HDL: high-density lipoprotein

VLDL: very low-density lipoprotein

LDLR: LDL receptor

VLDLR: VLDL receptor

RA: rheumatoid arthritis

CIA: collagen type II-induced arthritis

CVD: cardiovascular disease

Col II: collagen type II

CFA: complete Freund's adjuvant

TLR: toll-like receptor

DAMP: endogenous danger-associated molecular pattern

WT: wild type

B6: C57BL/6

NCD: normal chow diet

HCD: atherogenic hypercholesterolemic diet

PON-1: paraoxanase

U/ml: titration units/ml

RT-qPCR: quantitative real time reverse transcriptase PCR

IL-1β: interleukin-1β

TNFα: tumor necrosis factor-α

SUMMARY

Apolipoprotein E (ApoE) deficiency promoted an exacerbation of autoimmune arthritis in mice by inducing pro-inflammatory immune responses. In this study we analysed the contribution of hypercholesterolemia and/or the absence of ApoE anti-inflammatory properties, unrelated to its function in the control of cholesterol metabolism, towards the acceleration of arthritis in these mutant animals. The induction and severity of collagen type II-induced arthritis (CIA) were compared for B10.RIII wild type (WT), B10.RIII.*ApoE*$^{+/-}$, B10.RIII.*ApoE*$^{-/-}$ and B10.RIII.*LDLR*$^{-/-}$ mice with different concentrations of circulating ApoE and cholesterol. A 50-70% reduction in serum levels of ApoE was observed in heterozygous B10.RIII.*ApoE*$^{+/-}$ mice in comparison to B10.RIII.WT, although both strains of mice exhibited similar circulating lipid profiles. This ApoE reduction was associated with an increased CIA severity that remained lower than in homozygous B10.RIII.*ApoE*$^{-/-}$ mice. An important rise in circulating ApoE concentration was observed in hypercholesterolemic B10.RIII.*LDLR*$^{-/-}$ mice fed with a normal chow diet, and both parameters further increased with an atherogenic hypercholesterolemic diet. However the severity of CIA in B10.RIII.*LDLR*$^{-/-}$mice was similar to that of B10.RIII.WT controls. In conclusion, by comparing the evolution of CIA between several strains of mutant mice with different levels of serum ApoE and cholesterol, our results demonstrate that both hypercholesterolemia and ApoE regulate the intensity of in vivo systemic autoimmune responses.

INTRODUCTION

Rheumatoid arthritis (RA) is a chronic autoimmune disease resulting in joint inflammation and destruction. A strong association between RA and an increased risk of cardiovascular disease (CVD), due to accelerated atherosclerosis, has been established (1, 2). In this regard, different studies show that dyslipidemia is highly prevalent in patients with RA and may be present at least 10 years before the onset of the disease (3-5). However, a relationship between an altered lipid profile in plasma and the augmented incidence of CVD in RA patients has not been clearly proven and is still the subject of intense debate (6, 7).

On the other hand, dyslipidemia can trigger or potentiate already existing inflammatory responses and thereby enhance the severity of RA. Oxidized low-density lipoproteins (oxLDL) that accumulate in the macrophages of the arterial intima during hypercholesterolemia are good activators of toll-like receptor 4 (TLR4), acting as endogenous danger-associated molecular patterns (DAMP) (8). Also, it has been reported that in T cells from systemic lupus erythematosus patients, dyslipidemia may potentiate antigen receptor signalling through the increase of glycosphingolipid synthesis and their incorporation into membrane lipid rafts (9). Accordingly, a relationship between hypercholesterolemia and RA severity has been established (10) although it has not been confirmed by others (11).

Experimental animal models of RA in association with dyslipidemia constitute excellent tools to explore some of above mentioned questions. In this regard, we and others have recently shown that ApoE (*ApoE*$^{-/-}$) deficiency exacerbates the development of collagen type II (col II)-induced autoimmune arthritis (CIA) in B10.RIII mice in association with enhanced Th1 and Th17 inflammatory responses (12) or the semi-chronic K/BxN serum transfer-induced inflammatory arthritis through the potentiation

of innate immune responses (13). Accordingly, these experimental models can be used to explore whether the accelerated arthritis observed in *ApoE*$^{-/-}$ is related to the hypercholesterolemia characteristic of these mutant mice and/or to the lack of some of the previously identified anti-inflammatory properties of ApoE, that are unrelated to its function in the control of cholesterol metabolism (14). In the present study, we have explored these questions comparing the severity of CIA between mice expressing different amounts of ApoE in the context of either normal or altered circulating cholesterol levels.

MATERIALS AND METHODS

Mice.

C57BL/6.*ApoE*$^{-/-}$ (B6.*ApoE*$^{-/-}$, H-2^{b}) and B10.RIII (H-2^{r}) mice were purchased from Charles River (Barcelona, Spain) and Harlan Iberica (Barcelona, Spain), respectively. B6 mice deficient in LDL receptor (B6.*LDLR*$^{-/-}$) were kindly provided by Dr. Jorge Joven, Unitat de Recerca Biomèdica, Hospital Universitari Sant Joan, Institut d'Investigació Sanitària Pere Virgili, Universitat Rovira i Virgili, Reus, Spain. B10.RIII.*ApoE*$^{-/-}$ mice were obtained from our animal facilities as described recently (12) and intercrossed with B10.RIII wild type (B10.RIII.WT) mice to obtain B10.RIII.*ApoE*$^{-/-}$, B10.RIII.*ApoE*$^{+/-}$ and B10.RIII.WT littermates. B10.RIII.*LDLR*$^{-/-}$mice were produced in our animal facilities by backcrossing B6.*LDLR*$^{-/-}$ mice with B10.RIII mice for 7 backcross generations. In the second backcross generation, H-2$^{r/r}$ mice were selected by flow cytometry using specific mAbs against H-2^{b} and H-2^{r} (BD Biosciences, Madrid, Spain). In the last backcross generation, male and female heterozygous mice were intercrossed and B10.RIII.*LDLR* and B10.RIII.WT littermates were selected by PCR of genomic DNA extracted from mouse tails. Mice were fed ad

libitum with a normal chow diet (NCD) or an atherogenic hypercholesterolemic diet (HCD) (10.8% total fat, 0.75% cholesterol, S4892-E010, Ssniff, Germany) and bled from the retro-orbital plexus 4 weeks after immunization. All animal care and experimental procedures were carried out according to institutional guidelines and approved by the Universidad de Cantabria Institutional Laboratory Animal Care and Use Committee (ref 2014/12).

Induction and assessment of arthritis.

Bovine col II (MD Bioproducts, Zürich, Switzerland), dissolved at a concentration of 2 mg/ml in 0.05 M acetic acid, was emulsified with CFA containing 4 mg/ml of *Mycobacterium tuberculosis* (MD Bioproducts). For the induction of CIA, 8-12 week-old male mice were immunized once at the base of the tail with 150 µg of antigen in a final volume of 150 µl. A clinical evaluation of arthritis severity was performed as described (15).

Radiological studies were performed using a CCX Rx ray source of 70 Kw with an exposition of 90 ms (Trophy Irix X-Ray System; Kodak Spain, Madrid) and Trophy RVG Digital Imagining system as previously described (15). Radiological images were scale-graded according to the presence of 4 different radiological lesions (1: soft tissue swelling, 2: juxta-articular osteopenia due to alterations in bone density, 3: joint space narrowing or disappearance, and 4: bone surface irregularities due to marginal erosions and/or periosteal new bone formation). The extension of every individual lesion in each paw (local: affecting one digit or one joint in the carpus; diffuse: affecting two or more digits and/or two or more joints in the carpus) was graded from 0 to 2 as follows: 0: absence; 1: local; 2: diffuse.

Flow cytometry studies.

Spleen cells from B10.RIII.WT, B10.RIII.*ApoE*$^{+/-}$ and B10.RIII.*ApoE*$^{-/-}$ mice were stimulated in vitro with concanavalin A (Sigma-Aldrich, St Louis, MO) at a concentration of 5 µg/ml or with plastic-bound anti-CD3 (1 µg/well) and anti-CD28 (0.5 µg/well) mAbs (αCD3/αCD28). The induction of the CD69 and CD25 activation markers in CD4^{+} cells was analysed after 3 and 12 hrs of stimulation by flow cytometry using commercially labeled antibodies (Biolegend, London, United Kingdom).

Two-month old B10.RIII.WT, B10.RIII.*ApoE*$^{+/-}$ and B10.RIII.*ApoE*$^{-/-}$ mice were injected ip with 10 µg of LPS (Sigma-Aldrich) or with PBS as a control. Peritoneal cells were harvested 2 days later and the M1 (CD11b^{+}F4/80^{+}MHC-II^{+}) and M2 (CD11b^{+}F4/80^{+}CD206^{+}) macrophages characterized by flow cytometry. Cells were analyzed in a FACSCanto II flow cytometer using FACSDiva software (BD Biosciences).

Serological studies.

Total cholesterol (TC), high-density lipoprotein-cholesterol (HDL-c), LDL/VLDL-c and triglyceride levels in serum samples were determined using an autoanalyzer (Biosystems SA, Barcelona, Spain) following manufacturer instructions. Serum levels of IgG1 and IgG2a anti-col II antibodies were measured by ELISA as described (12). Results were expressed in titration units/ml (U/ml) in reference to a standard curve obtained from a serum pool of col II-CFA immunized DBA/1 mice. Circulating levels of ApoE were determined by ELISA as described (16). Briefly, microtiter plates (Maxisorp Nunc-immuno plates, ThermoFisher Scentific, Waltham, MA) were coated with 0.1 µg/ml of WUE-4 (mouse anti-human ApoE mAb, Novus Biologicals, Madrid, Spain) and the assay was developed with goat anti-mouse ApoE

(Merck Millipore, Madrid, Spain) followed by a biotinylated rabbit anti-goat antibody (Vector Laboratories Burlingame, CA) and streptavidin-alkaline phosphatase (BD Biosciences). Results were expressed in µg/ml in reference to a standard curve obtained with purified mouse ApoE (a kind gift of Dr. Karl Weisgraber, Gladstone Institute of Neurological Disease, University of California San Francisco, CA).

Mouse HDL from each group was isolated by sequential ultracentrifugation at 100 000 × g for 24 h at a density of 1.063–1.21 g/ml. HDL composition, including total and free cholesterol, triglycerides and phospholipids, was determined by commercial methods adapted to the Hitachi 917 autoanalyzer (Roche Diagnostics, Rotkreuz, Switzerland). HDL protein concentrations were determined by the bicinchoninic acid method (Termo Scientific, Rockford, IL). The ability of HDL to protect against LDL oxidation was determined on an assay in which human LDL (0.1mM phospholipids) was oxidized alone with 2.5 µM $CuSO_4$ or in the presence of equal concentrations of HDL phospholipids from each experimental group (0.1mM phospholipids). The oxidation kinetics were followed through continuous monitoring of the formation of conjugated diene at 37ºC for 4h (17). The kinetics of LDL in the LDL + HDL incubations were calculated by subtracting the kinetics of HDL incubated without LDL. The lag phases were calculated and the results represented as relative lag phase to the LDL kinetics oxidized without HDL. (17). Paraoxonase (PON)-1 was measured using phenylacetate as substrate (17).

Cytokine expression.

The expression of mRNAs encoding for interleukin-1β (IL-1β), tumor necrosis factor-α (TNFα), IL-6, transforming growth factor-β (TGFβ) and IL-10 cytokines was explored in the paws before col II immunization and 8 weeks after using quantitative

real time reverse transcriptase PCR (RT-qPCR). After skin removal, the paws were kept frozen at -70 ºC until processing. Total RNA from powdered paws was obtained by TRIzol extraction (Invitrogen, ThermoFisher Scentific). One µg of the isolated RNA was used for cDNA synthesis with a RT-PCR kit (Bio-Rad Laboratories, Madrid, Spain), according to manufacturer instructions. Quantitative real time PCR (RT-qPCR) was performed on a StepOne Plus real time PCR instrument (Applied Biosystems, ThermoFisher Scentific) using specific TaqMan expression assays and a universal PCR Master Mix (Applied Biosystems, ThermoFisher Scentific). Results (in triplicate) were normalized to *GAPDH* expression and measured in parallel for each sample.

Statistical analysis.

The differences between the two groups were analyzed by a 2-tailed Student's *t* or 2-sample Mann-Whitney *U* tests. Probability values <0.05 were considered significant.

RESULTS

The severity of CIA in *ApoE* mutant mice directly correlates with the levels of circulating ApoE.

We and others have recently reported the development of an exacerbated inflammatory arthritis in mice deficient in ApoE (12, 13). To analyze whether the enhanced disease in these mutant mice was related to the hypercholesterolemia and/or to the absence of ApoE, we compared the development of CIA between B10.RIII.WT, B10.RIII.*ApoE*$^{+/-}$ and B10.RIII.*ApoE*$^{-/-}$ mice. Serum ApoE levels and lipid profiles were first analyzed in the different experimental groups. The levels of circulating ApoE in heterozygous B10.RIII.*ApoE*$^{+/-}$ mice were approximately one-third/half of those found

in B10.RIII.WT, both before and after col II immunization (Figure 1A). A significant reduction in the levels of circulating TC and HDL-c, but not of LDL/VLDL-c and triglycerides, was observed in B10.RIII.WT mice in association with the development of CIA (Figure 1B; $p<0.05$ in both cases). Despite the reduced ApoE concentration, the levels of circulating TC, HDL-c, LDL/VLDL-c and triglycerides in B10.RIII.*ApoE*$^{+/-}$ before immunization were normal and similar to those of non-immunized B10.RIII.WT mice (Figure 1B). Again, reduced levels of circulating TC and HDL-c ($p<0.05$ and $p<0.01$, respectively) were detected in B10.RIII.*ApoE*$^{+/-}$ after immunization with col II, and these levels remained similar to those of immunized B10.RIII.WT controls (Figure 1B). As expected, ApoE was undetectable in sera from non-immunized and col II-immunized B10.RIII.*ApoE*$^{-/-}$ mice, along with the presence of an abnormal lipid profile characterized by increased levels of triglycerides, TC and LDL/VLDL-c ($p<0.001$ in all cases) and normal levels of HDL-c (Figure 1A and B), in comparison to both B10.RIII.WT and B10.RIII.*ApoE*$^{+/-}$ mice.

As previously described (12), the severity of CIA in B10.RIII.*ApoE*$^{-/-}$ mice was higher than in B10.RIII.WT mice (Figure 2). In inverse correlation with serum levels of ApoE, the clinical severity of CIA in B10.RIII.*ApoE*$^{+/-}$ mice was also significantly higher than in B10.RIII.WT controls but lower than in B10.RIII.*ApoE*$^{-/-}$ mice (Figure 2A). This was confirmed by analyzing different radiological signs associated with bone and cartilage damage. The extent of joint narrowing or disappearance of the interosseous spaces, reflecting cartilage loss, and of bone irregularities, secondary to periosteal new bone formation and/or marginal articular erosions, was higher in B10.RIII.*ApoE*$^{-/-}$ than in B10.RIII.*ApoE*$^{+/-}$ mice (Figure 2B and C). Although the degree of soft tissue swelling and of juxta-articular osteopenia was also slightly larger in B10.RIII.*ApoE*$^{-/-}$ than in B10.RIII.*ApoE*$^{+/-}$ mice, these increases were not statistically

significant. The severity of all radiological signs was significantly lower in B10.RIII.WT controls than in B10.RIII.*ApoE*$^{+/-}$ and B10.RIII.*ApoE*$^{-/-}$ mice (Figure 2B and C).

The accelerated disease in B10.RIII.*ApoE*$^{-/-}$ mice was shown to correlate with qualitative changes in anti-col II humoral immune responses and with an enhanced gene expression of arthritogenic cytokines in the paws (12). To explore whether similar abnormalities also accounted for the aggressive disease progression in heterozygous B10.RIII.*ApoE*$^{+/-}$ mice, circulating levels of IgG1 and IgG2a anti-col II antibodies were first compared in the different experimental groups before CIA induction and 4 weeks after. As reported (12), the circulating levels of IgG1 anti-col II antibodies were significantly reduced in immunized B10.RIII.*ApoE*$^{-/-}$ mice in comparison to both B10.RIII.WT and B10.RIII.*ApoE*$^{+/-}$ mice (Figure 3A). Although the levels of IgG1 anti-col II antibodies also tended to decrease in immunized B10.RIII.*ApoE*$^{+/-}$ in comparison to B10.RIII.WT controls, these differences did not reach statistical significance (Figure 3A; p= 0.07). No changes in the titers of serum IgG2a anti-col II antibodies were observed between the different experimental groups (Figure 3A).

A significant increased expression of arthritogenic IL-1β, TNFα and IL-6 mRNAs was observed in the paws of B10.RIII.*ApoE*$^{-/-}$ in comparison to B10.RIII.WT mice 8 weeks after immunization with col II-CFA (Figure 3B). In B10.RIII.*ApoE*$^{+/-}$ mice, the expression of IL-1β and TNFα, but not IL-6, mRNAs in the paws was also augmented during CIA in comparison to B10.RIII.WT mice (Figure 3B). No changes in the expression of the anti-inflammatory cytokines TGFβ and IL-10 were observed among the different groups of immunized mice (Figure 3B).

Different studies indicated that ApoE influenced the in vitro activation of T cells and the macrophage polarization into pro-inflammatory M1 cells (18, 19). We then

assessed whether the enhanced CIA observed in B10.RIII.*ApoE*$^{+/-}$ and B10.RIII.*ApoE*$^{-/-}$ mice correlated with an abnormal T-cell activation and/or an enhanced M1 macrophage polarization. No differences in the kinetics of CD69 and CD25 induction were observed in $CD4^+$ cells from the different strains of mice after concanavalin A or αCD3/αCD28 stimulation (Figure 4A). However, an altered peritoneal macrophage polarization, characterized by an increased M1 polarization and a reduced M2 polarization, was observed in B10.RIII.*ApoE*$^{-/-}$ mice 48 hours after ip injection of LPS in comparison to B10.RIII.WT controls (Figure 4B). Again, an intermediate phenotype was observed in heterozygous B10.RIII.*ApoE*$^{+/-}$ mice after LPS treatment (Figure 4B).

Functional properties of HDL in ApoE mutant mice.

ApoE is a component of HDL particles (20). In addition, chronic inflammation has been shown to alter the anti-inflammatory properties of HDLs transforming them into pro-inflammatory molecules (20, 21). Therefore, we next explored whether the reduction or absence of ApoE and/or the exacerbated CIA observed in B10.RIII.*ApoE*$^{+/-}$ and B10.RIII.*ApoE*$^{-/-}$ mice induced functional changes in these lipoproteins. An assessment of the lipid and protein composition of HDLs obtained from each mouse genotype revealed significant increases in the distribution of free and esterified cholesterol as well as an increase in the percentage of proteins and a reduction in PON-1 activity in B10.RIII.*ApoE*$^{-/-}$ mice (Table 1). With the exception of a moderate but significant increase in the percentage of proteins, the biochemical composition of HDLs from B10.RIII.*ApoE*$^{-/-}$ mice was similar to that of B10.RIII.WT mice (Table 1).

The ability of HDLs, purified from serum pools of col II immunized B10.RIII.WT, B10.RIII.*ApoE*$^{+/-}$ or B10.RIII.*ApoE*$^{-/-}$ mice, to inhibit the oxidation of human LDLs in the presence of $CuSO_4$ was then analyzed. Despite the biochemical

differences in the composition of HDLs between B10.RIII.*ApoE*$^{-/-}$ mice and B10.RIII.WT and B10.RIII.*ApoE*$^{+/-}$ mice, these particles showed a similar anti-oxidant capacity in all the experimental groups (Table 1).

Lack of exacerbation of CIA in hypercholesterolemic B10.RIII.*LDLR*$^{-/-}$ mice in association with the increase in serum ApoE levels.

Although our present observations in B10.RIII.*ApoE*$^{+/-}$ mice are compatible with an immunosuppressive activity of ApoE in vivo, independently of its role in cholesterol metabolism, these results cannot formally exclude the participation of hypercholesterolemia in the aggravation of CIA in B10.RIII.*ApoE*$^{-/-}$ mice. To further explore this issue we used B10.RIII.*LDLR*$^{-/-}$ mice. As previously reported (22), these mice exhibited increased levels of TC and LDL/VLDL-c in sera when fed with a NCD and these levels were even higher under a HCD (Figure 5A: $p<0.001$ in all cases). These abnormal circulating lipid profiles of B10.RIII.*LDLR*$^{-/-}$ mice were similar before and after CIA induction (Figure 5A). In association with the presence of hypercholesterolemia, very high levels of circulating ApoE were found in B10.RIII.*LDLR*$^{-/-}$ mice fed with NCD and these levels increased with the HCD, both before and after CIA induction (Figure 5B). A significant reduction in circulating TC and HDL-c, but not LDL/VLDL-c, concentrations was again observed in B10.RIII.WT mice fed with a NCD, but not with a HCD, during the development of CIA, (Figure 5A). In these WT mice, the type of diet had no effect on serum levels of ApoE neither before nor after col II immunization (Figure 5B).

Regardless of the diet received, no significant differences in the severity of clinical and radiological signs were observed between B10.RIII.*LDLR*$^{-/-}$ and B10.RIII.WT mice after CIA induction that were lower than in B10.RIII.*ApoE*$^{-/-}$ mice (Figure 6 A-C). Similarly, paw expression of IL-1β, TNFα and IL-6 mRNAs was

significantly lower in B10.RIII.*LDLR*$^{-/-}$ and B10.RIII.WT mice than in B10.RIII.*ApoE*$^{-/-}$ mice 8 weeks after col II immunization (Figure 6D). Again, the expression of TGFβ and IL-10 was similar in the different groups of mice after CIA induction (data not shown).

DISCUSSION

The deficiency of ApoE has recently been shown to exacerbate disease severity in two experimental models of autoimmune arthritis in mice by inducing inflammatory immune responses (12, 13). However, the underlying mechanisms by which an ApoE deficiency promotes such immunological abnormalities have not been clarified. Using either normocholesterolemic or hypercholesterolemic mice with different concentrations of circulating ApoE, we have demonstrated here that both the hypercholesterolemia and the deficiency in ApoE cooperate towards the worsening of CIA in B10.RIII.*ApoE*$^{-/-}$ mice.

While an association between RA and increased risk of atherosclerosis and CVD has been strongly established (1, 2), there exist controversies regarding the importance of dyslipidemia in this association (3-7). Furthermore, some studies indicate that abnormal lipid profiles in sera, defined as high levels of TC and triglycerides and lower HDL-c levels, were present in more than 50% of patients with RA before or after disease diagnosis (3-5). In contrast, studies show that a significant fraction of RA patients exhibit decreased levels of TC and LDL-c and normal values of HDL-c, reflecting what has been called the lipid paradox in RA (6, 7). Although the reasons for these discrepancies have not been exactly determined, they can be related to differences in the inflammatory status of the patients and/or in their dietary habits among the different studies. In this regard, we show here that the development of CIA in both B10.RIII.WT and B10.RIII.*ApoE*$^{+/-}$ mice is associated with a reduction in serum levels

of TC and HDL-c, but not of LDL/VLDL-c and triglycerides, when fed using NCD, but not HCD. Furthermore, inflammation or infection has been reported to alter lipid profiles in sera, as observed in mice with sepsis (23).

Previous observations demonstrate that small amounts of ApoE are sufficient to normalize plasma cholesterol levels and to inhibit atherosclerosis in mice (24, 25). In our present study, we show an aggravation of CIA in B10.RIII.*ApoE*$^{+/-}$ mice having 30-50% of the circulating ApoE observed in WT mice but normal cholesterol profiles. Independently of these dose-dependent differences, that may be related to the degree of systemic inflammation in each experimental model, both studies highlight the anti-inflammatory role of ApoE in vivo that is unrelated of its activity in the control of cholesterol metabolism. The anti-inflammatory activity of ApoE has been demonstrated in several studies. ApoE-containing lipoproteins are very efficient suppressing mitogen-induced proliferative responses of T lymphocytes by reducing the production of IL-2 (18). ApoE also regulates the TLR4- and TLR3-mediated production of IL-12 (26) and prevents the LPS-induced production of cytokines and subsequent death in rodents (27). Furthermore, an ectopic ApoE expression in macrophages and monocytes from *ApoE*$^{-/-}$ mice suppresses nuclear factor-κB-mediated inflammation by enhancing miR-146a levels (28). In this regard, our results indicate that the partial or total ApoE deficiency modifies the polarization of macrophages after a potent inflammatory insult in vivo but has no effect on the in vitro activation of $CD4^+$ cells. The anti-inflammatory capacity of ApoE appears to be isoform-dependent, and animals expressing the E4 allele have greater inflammatory responses (29). Interestingly, there is one study that shows an association between the ApoE4 genotype and bone loss in human RA (30), although it has not been confirmed by other authors (31). The similarities observed in the anti-col II antibody responses and in the pattern of cytokine expression in the paws during CIA

development between B10.RIII.*ApoE*$^{+/-}$ and B10.RIII.*ApoE*$^{-/-}$ mice suggest that common mechanisms are responsible for the accelerated diseases in both strains of mice.

We show here that the biochemical composition of HDL particles differs between B10.RIII.*ApoE*$^{-/-}$ and WT controls, with an increase and reduction in the amount of free and esterified cholesterol in HDLs from mutant mice, respectively. Although the molecular basis of this alteration is unknown, it can be related to changes in the expression and/or function of the lecithin:cholesterol acyltransferase, an enzyme involved in the conversion of phosphatidylcholine and cholesterol into cholesteryl ester and lysophosphatidylcholine in plasma and other biological fluids (32). However, these differences do not modify their ability to protect against LDL oxidation. This, together with the fact that the biochemical composition of HDLs and their in vitro anti-oxidant activity are similar in B10.RIII.*ApoE*$^{+/-}$ and B10.RIII.WT mice, strongly suggests that the exacerbation of arthritis observed in ApoE mutant mice is largely independent of HDL function. However, since our HDL experiments have been performed in a cell-free system, we cannot completely rule out some direct pro-inflammatory effects of HDLs in B10.RIII.*ApoE*$^{-/-}$ and B10.RIII.*ApoE*$^{+/-}$ mice.

The link between cholesterol homeostasis and immune system activation has been extensively documented in recent years (reviewed in 33). To directly analyze the importance of hypercholesterolemia in the control of CIA severity, we have employed B10.RIII.*LDLR*$^{-/-}$ mice. However, the increase in the levels of circulating cholesterol in these mice also promotes an important rise in serum ApoE concentration that according to previous studies, probably reflects a liver X receptor-dependent adaptive response to cholesterol overload (34). In agreement with the observations in B10.RIII.*ApoE*$^{+/-}$ mice, the high levels of ApoE in B10.RIII.*LDLR*$^{-/-}$ mice could initially anticipate a reduction in the severity of CIA in these animals. Nevertheless, the absence of such protection is

compatible with a role for hypercholesterolemia as an additional worsening factor for CIA severity in B10.RIII.*ApoE*$^{-/-}$ mice. In this regard, oxLDL and cholesterol crystals can act as DAMPs in the macrophages that infiltrate the arterial intima during hypercholesterolemia, activating TLR4 and NLRP3 inflammasome signalling pathways, respectively (8, 35). Also, hypercholesterolemia can increase the content of lipid rafts in the plasma membrane, potentiating antigen receptor signalling in T cells (9).

ApoE binds to members of the LDLR family, including the LDLR, LDLR-related protein 1, VLDL receptor (VLDLR) and APOE receptor 2 (36) and several of these receptors have been involved in the anti-inflammatory effect of ApoE (19, 37). The fact that the severity of CIA in B10.RIII.*LDLR*$^{-/-}$ mice is lower than in B10.RIII.*ApoE*$^{-/-}$ mice indicates that LDLR is not the main receptor by which ApoE modulates CIA severity. Additional experiments are required to clarify the receptor/s involved in this protective activity of ApoE. In summary, our present results underline the important role played by ApoE and cholesterol in the regulation of inflammatory responses during the development of inflammatory arthritis and highlight the importance of these factors as potential relevant targets for the control of autoimmune disorders.

ACKNOWLEDGEMENTS

We thank Dr. Jorge Joven, Unitat de Recerca Biomèdica, Hospital Universitari Sant Joan, Institut d'Investigació Sanitària Pere Virgili, Universitat Rovira i Virgili, Reus, Spain for the B6.*LDLR*$^{-/-}$ mice and Dr. Karl Weisgraber, Gladstone Institute of Neurological Disease, University of California San Francisco, CA for the purified mouse ApoE. We also thank María Aramburu, Natalia Cobo and Iván Gómez for their technical assistance. This work was supported by grants from the Spanish Ministerio de

Economía y Competitividad to JM (SAF2012-34059) and RM (SAF2014-55088-R), which were co-funded by the European Regional Development Fund. MI was partially supported by a grant from the Spanish Ministerio de Economía y Competitividad (IPT2011-1527-010000) associated with Fibrostatin SL. PA performed the majority of experiments, analyzed the data and wrote the manuscript, FG carried out arthritis experiments in B10.RIII.*ApoE*$^{+/-}$ mice, MI, JJA and ET performed the titration of anti-col II antibodies, the RNA isolation from the paws and the RT-qPCR studies, FB-V and JCE-G purified HDL from serum pools and characterized their biochemical properties and anti-oxidative activities in vitro, BL performed the cholesterol profiles in sera and JM and RM conceived and designed the experiments, analyzed the data and wrote the manuscript.

COMPETING INTERESTS

The authors declare no competing financial interests.

REFERENCES

1. John H, Kitas G. Inflammatory arthritis as a novel risk factor for cardiovascular disease. Eur J Intern Med. 2012; 23:575-9.
2. Young A, Koduri G, Batley M, et al. Mortality in rheumatoid arthritis. Increased in the early course of disease, in ischaemic heart disease and in pulmonary fibrosis. Rheumatology. 2007; 46:350-7.
3. Dessein PH, Joffe BI, Veller MG, Stevens BA, Tobias M, Reddi K, Stanwix AE. Traditional and nontraditional cardiovascular risk factors are associated with atherosclerosis in rheumatoid arthritis. J Rheumatol. 2005; 32:435-42.

4. Park YB, Lee SK, Lee WK, Suh CH, Lee CW, Lee CH, Song CH, Lee J. Lipid profiles in untreated patients with rheumatoid arthritis. J Rheumatol. 1999; 26:1701-4.

5. van Halm VP, Nielen MM, Nurmohamed MT, et al. Lipids and inflammation: serial measurements of the lipid profile of blood donors who later developed rheumatoid arthritis. Ann Rheum Dis. 2007; 66:184-8.

6. Myasoedova E, Crowson CS, Kremers HM, Roger VL, Fitz-Gibbon PD, Therneau TM, Gabriel SE. Lipid paradox in rheumatoid arthritis: the impact of serum lipid measures and systemic inflammation on the risk of cardiovascular disease. Ann Rheum Dis. 2011; 70:482-7.

7. Bag-Ozbek A, Giles JT. Inflammation, adiposity, and atherogenic dyslipidemia in rheumatoid arthritis: is there a paradoxical relationship? Curr Allergy Asthma Rep. 2015;15:497.

8. Imai Y, Kuba K, Neely GG, et al. Identification of oxidative stress and Toll-like receptor 4 signaling as a key pathway of acute lung injury. Cell. 2008; 133: 235-49.

9. McDonald G, Deepak S, Miguel L, Hall CJ, Isenberg DA, Magee AI, Butters T, Jury EC. Normalizing glycosphingolipids restores function in CD4+ T cells from lupus patients. J Clin Invest. 2014; 124:712-24.

10. Lazarevic MB, Vitic J, Mladenovic V, Myones BL, Skosey JL, Swedler WI. Dyslipoproteinemia in the course of active rheumatoid arthritis. Semin Arthritis Rheum. 1992; 22:172-8.

11. Daoussis D, Panoulas VF, Antonopoulos I, et al. Cardiovascular risk factors and not disease activity, severity or therapy associate with renal dysfunction in patients with rheumatoid arthritis. Ann Rheum Dis. 2010; 69:517-21.

12. Postigo J, Genre F, Iglesias M, Fernández-Rey M, Buelta L, Carlos Rodríguez-Rey J, Merino J, Merino R. Exacerbation of type II collagen-induced arthritis in apolipoprotein E-deficient mice in association with the expansion of Th1 and Th17 cells. Arthritis Rheum. 2011; 63:971-80.
13. Archer AM, Saber R, Rose S, et al. ApoE deficiency exacerbates the development and sustainment of a semi-chronic K/BxN serum transfer-induced arthritis model. J Transl Med. 2016; 14:170.
14. Raffai RL. Apolipoprotein E regulation of myeloid cell plasticity in atherosclerosis. Curr Opin Lipidol. 2012; 23:471-8.
15. González J, Tamayo E, Santiuste I, et al. $CD4^{+}CD25^{+}$ T cell-dependent inhibition of autoimmunity in transgenic mice overexpressing human Bcl-2 in T lymphocytes. J Immunol. 2007; 178:2778-86.
16. Hirsch-Reinshagen V, Donkin J, Stukas S, et al. LCAT synthesized by primary astrocytes esterifies cholesterol on glia-derived lipoproteins. J Lipid Res. 2009; 50:885-93.
17. Escolà-Gil JC, Chen X, Julve J, et al. Hepatic lipase- and endothelial lipase-deficiency in mice promotes macrophage-to-feces RCT and HDL antioxidant properties. Biochim Biophys Acta. 2013; 1831:691-7.
18. Kelly ME, Clay MA, Mistry MJ, Hsieh-Li H-M, Harmony JAK. Apolipoprotein E inhibition of proliferation of mitogen-activated T lymphocytes: production of interleukin 2 with reduced biological activity. Cell Immunol. 1994; 159:124-39.
19. Baitsch D, Bock HH, Engel T, et al. Apolipoprotein E induces antiinflammatory phenotype in macrophages. Arterioscler Thromb Vasc Biol. 2011; 31:1160-8.
20. Zhu X, Parks JS. New roles of HDL in inflammation and hematopoiesis. Annu Rev Nutr. 2012; 32:161-82.

21. McMahon M, Grossman J, FitzGerald J, et al. Proinflammatory high-density lipoprotein as a biomarker for atherosclerosis in patients with systemic lupus erythematosus and rheumatoid arthritis. Arthritis Rheum. 2006; 54:2541-9.

22. Osuga J, Yonemoto M, Yamada N, et al. Cholesterol lowering in low density lipoprotein receptor knockout mice overexpressing apolipoprotein E. J Clin Invest. 1998; 102:386-94.

23. Alvarez C, Ramos A. Lipids, lipoproteins, and apoproteins in serum during infection. Clin Chem. 1986; 32:142-5.

24. Linton MF, Atkinson JB, Fazio S. Prevention of atherosclerosis in apolipoprotein E-deficient mice by bone marrow transplantation. Science. 1995; 267:1034-7.

25. Zhu Y, Bellosta S, Langer C, Bernini F, Pitas RE, Mahley RW, Assmann G, Eckardstein A. Low-dose expression of a human apolipoprotein E transgene in macrophages restores cholesterol efflux capacity of apolipoprotein E-deficient mouse plasma. Proc Natl Acad Sci USA. 1998; 95:7585-90.

26. Ali K, Middleton M, Puré E, Rader DJ. Apolipoprotein E suppresses the type I inflammatory response in vivo Circ Res. 2005; 97:922-7.

27. Van Oosten M, Rensen PC, Van Amersfoort ES, et al. Apolipoprotein E protects against bacterial lipopolysaccharide-induced lethality. A new therapeutic approach to treat gram-negative sepsis. J Biol Chem. 2001; 276:8820-4.

28. Li K, Ching D, Luk FS, Raffai RL. Apolipoprotein E enhances microRNA-146a in monocytes and macrophages to suppress nuclear factor-κB-driven inflammation and atherosclerosis. Circ Res. 2015; 117:e1-e11.

29. Lynch JR, Tang W, Wang H, Vitek MP, Bennett ER, Sullivan PM, Warner DS, Laskowitz DT. APOE genotype and an ApoE-mimetic peptide modify the systemic

and central nervous system inflammatory response. J Biol Chem. 2003; 278:48529-33.

30. Lee SI, Lee SY, Yoo WH. Association of apolipoprotein E polymorphism with bone mineral density in postmenopausal women with rheumatoid arthritis. Rheumatology. 2005; 44:1067-8.
31. Maehlen MT, Provan SA, de Rooy DP, et al. Associations between APOE genotypes and disease susceptibility, joint damage and lipid levels in patients with rheumatoid arthritis. PLoS One. 2013; 8:e60970.
32. Jonas A. Lecithin cholesterol acyltransferase. Biochim Biophys Acta. 2000; 1529:245-56.
33. Fessler MB. Regulation of Adaptive Immunity in Health and Disease by Cholesterol Metabolism. Curr Allergy Asthma Rep. 2015; 15:48.
34. Bensinger SJ, Tontonoz P. Integration of metabolism and inflammation by lipid-activated nuclear receptors. Nature. 2008; 454:470-7.
35. Duewell P, Kono H, Rayner KJ, et al. NLRP3 inflammasomes are required for atherogenesis and activated by cholesterol crystals. Nature. 2010; 464:1357-61.
36. Huang Y, Mahley RW. Apolipoprotein E: structure and function in lipid metabolism, neurobiology, and Alzheimer's diseases. Neurobiol Dis. 2014; 72:3-12.
37. May P, Bock HH, Nofer JR. Low density receptor-related protein 1 (LRP1) promotes anti-inflammatory phenotype in murine macrophages. Cell Tissue Res. 2013; 354:887-9.

Table 1. HDL composition and anti-oxidant activity in *ApoE* mutant mice.

HDL characteristic	B10.RIII.WT	B10.RIII.*ApoE*$^{+/-}$	B10.RIII.*ApoE*$^{-/-}$
Esterified cholesterol (%)	18.0±3.5	15.4±3.1	9.8±3.4*†
Free cholesterol (%)	2.6±0.8	3.2±0.8	6.5±1.3*†
Phospholipids (%)	27.9±6.2	31.1±4.8	29.6±5.8
Triglycerides (%)	8.1±3.8	5.3±1.8	7.5±1.5
Protein (%)	43.3±0.4	45.0±1.3*	46.6±2.3*
PON1 activity (µmol/ml.min)	59.3±1.7	58.8±4.5	45.9±4.9*†
LDL oxidation protection (%)	175.2±8.8	185.1±49.3	167.9±12.1

HDL was isolated from plasma by sequential ultracentrifugation at 100,000 g for 24 h at a density of 1.063-1.21 g/ml, and lipids and protein were determined. Values are expressed as relative (%) chemical composition and correspond to HDL preparations isolated from four pooled samples of 4-6 mice in each group. Serum plasma arylesterase activity was measured using phenylacetate as substrate and EDTA-sensitive plasma arylesterase (PON1) activity was calculated by subtracting the EDTA-resistant arylesterase (5 animals/group). Human LDL was incubated with 2.5 µM CuSO4 in the presence or absence of purified HDLs (0.1mM phospholipids) from each mouse strain (3 purified pools of HDL/group). The percentage of protection of LDL oxidation is expressed as the mean ± SD. Values are mean ± SD. * P<0.05 versus B10.RIII.WT mice. † P<0.05 versus B10.RIII.*ApoE*$^{+/-}$ mice.

FIGURE LEGENDS

Figure 1: Serum lipid profiles and ApoE levels in *ApoE* mutant mice during CIA development. (A) Serum levels of ApoE in B10.RIII.WT, B10.RIII.*ApoE*$^{+/-}$ and B10.RIII.*ApoE*$^{-/-}$ mice before (NI) and 8 weeks after (Imm) induction of CIA determined by ELISA. (B) Serum levels of total cholesterol, HDLc, VLDL/LDLc and triglycerides in B10.RIII.WT, B10.RIII.*ApoE*$^{+/-}$ and B10.RIII.*ApoE*$^{-/-}$ mice before (NI) and 8 weeks after (Imm) induction of CIA. Representative results of 3 independent experiments are expressed as the mean ± SD (8-10 animals/group).Statistic differences are indicated as follow: ***p<0.005.

Figure 2: Development of CIA in *ApoE* mutant mice. 8-12 weeks-old B10.RIII.WT, B10.RIII.*ApoE*$^{+/-}$ and B10.RIII.*ApoE*$^{-/-}$ mice were immunized with col II-CFA. (A) Clinical severity of CIA in individual mice 8 weeks after immunization with col II. Bars represent the mean values. (B) Representative radiological images of the front paws from B10.RIII.WT, B10.RIII.*ApoE*$^{+/-}$ and B10.RIII.*ApoE*$^{-/-}$ mice before and 8 weeks after immunization with col II. (C) Severity score of individual radiological signs, expressed as the mean ± SD (n= 7-10 mice/group), 8 weeks after immunization. Bars represent the mean values. Results from A to C are representative of 4 independent experiments. Statistical differences are indicated as follows: ns: non-significant, *p<0.05, **p<0.01, ***p<0.005.

Figure 3: Anti-col II humoral responses and cytokine gene expression in *ApoE* mutant mice. (A) Serum levels of IgG1 and IgG2a anti-col II antibodies in individual mice before (NI) and 4 weeks after (Imm) immunization with col II. Bars represent the mean values. Results are representative of 2 independent experiments. (B) Analysis by

RT-qPCR of IL-1β, TNFα and IL-6 gene expression in the paws of B10.RIII.WT, B10.RIII.*ApoE*$^{+/-}$ and B10.RIII.*ApoE*$^{-/-}$ mice before (NI; closed bars) and 8 weeks after (Imm; open bars) immunization with col II. Representative results from one out three independent experiments (6-8 animals/group) are expressed as the mean ± SD fold change of each cytokine relative to GAPDH expression measured in parallel in each sample. Statistical differences are indicated as follows: ns: non-significant, *p<0.05, **p<0.01.

Figure 4: Effects of ApoE deficiency on the activation of CD4$^+$ cells and in M1/M2 macrophage polarization. (A) Spleen cells from B10.RIII.WT, B10.RIII.*ApoE*$^{+/-}$ and B10.RIII.*ApoE*$^{-/-}$ mice were stimulated in vitro with concanavalin A or with αCD3/αCD28, and the kinetics of CD69 and CD25 induction was analyzed by flow cytometry 3 and 12 hrs after. Results are expressed as overlapping representative histograms of B10.RIII.WT (thin line), B10.RIII.*ApoE*$^{+/-}$ (dotted line) and B10.RIII.*ApoE*$^{-/-}$ (thick line) mice in one of two independent experiments. (B) B10.RIII.WT, B10.RIII.*ApoE*$^{+/-}$ and B10.RIII.*ApoE*$^{-/-}$ mice were injected with PBS or LPS and the percentages of M1 and M2 macrophages in the peritoneal cavity analyzed by flow cytometry 48 hrs later. Representative results of 2 independent experiments are expressed as the mean ± SD (3-4 animals/group). Statistical differences are indicated as follows: ns: non-significant, *p<0.05.

Figure 5: Serum lipid profiles and ApoE levels in B10.RIII.*LDLR*$^{-/-}$ mice during CIA development. (A) Serum levels of total cholesterol, HDLc and VLDL/LDLc in B10.RIII.WT, B10.RIII.*LDLR*$^{-/-}$ and B10.RIII.*ApoE*$^{-/-}$ mice fed with a NCD or a HCD before and 8 weeks after induction of CIA. Representative results of 2 independent

experiments are expressed as the mean ± SD (8-10 animals/group). (B) Serum levels of ApoE in B10.RIII.WT, B10.RIII.*LDLR*$^{-/-}$ and B10.RIII.*ApoE*$^{-/-}$ mice fed with a NCD or a HCD before and 8 weeks after induction of CIA determined by ELISA. Statistical differences are indicated as follows: ns: non-significant, *p<0.05, **p<0.01.

Figure 6: Lack of exacerbation of CIA in B10.RIII.*LDLR*$^{-/-}$ mice. 8-12 weeks-old B10.RIII.WT, B10.RIII.*LDLR*$^{-/-}$ and B10.RIII.*ApoE*$^{-/-}$ mice fed with a NCD or a HCD were immunized with col II-CFA. (A) Clinical severity of CIA in individual mice 8 weeks after immunization with col II. Bars represent the mean values. (B) Representative radiological images of the front paws from mice before immunization with col II and 8 weeks after. (C) Severity score of individual radiological signs, expressed as the mean ± SD (n= 6-8 mice/group), 8 weeks after immunization. Bars represent the mean values. Results from A to C are representative of 3 independent experiments. (D) Expression of IL-1β, TNFα and IL-6 mRNAs by RT-qPCR in the paws of the mice fed with NCD (open bars) or HCD (closed bars) 8 weeks after (Imm) immunization with col II. For each cytokine analysis, a mixed group of non-immunized (NI) mice is included for comparison. Representative results from one out three independent experiments (5-9 animals/group) are expressed as mean ± SD fold change of each cytokine relative to GAPDH expression measured in parallel in each sample. Statistical differences are indicated as follows: ns: non-significant, *p<0.05, **p<0.01, *** p<0.005.

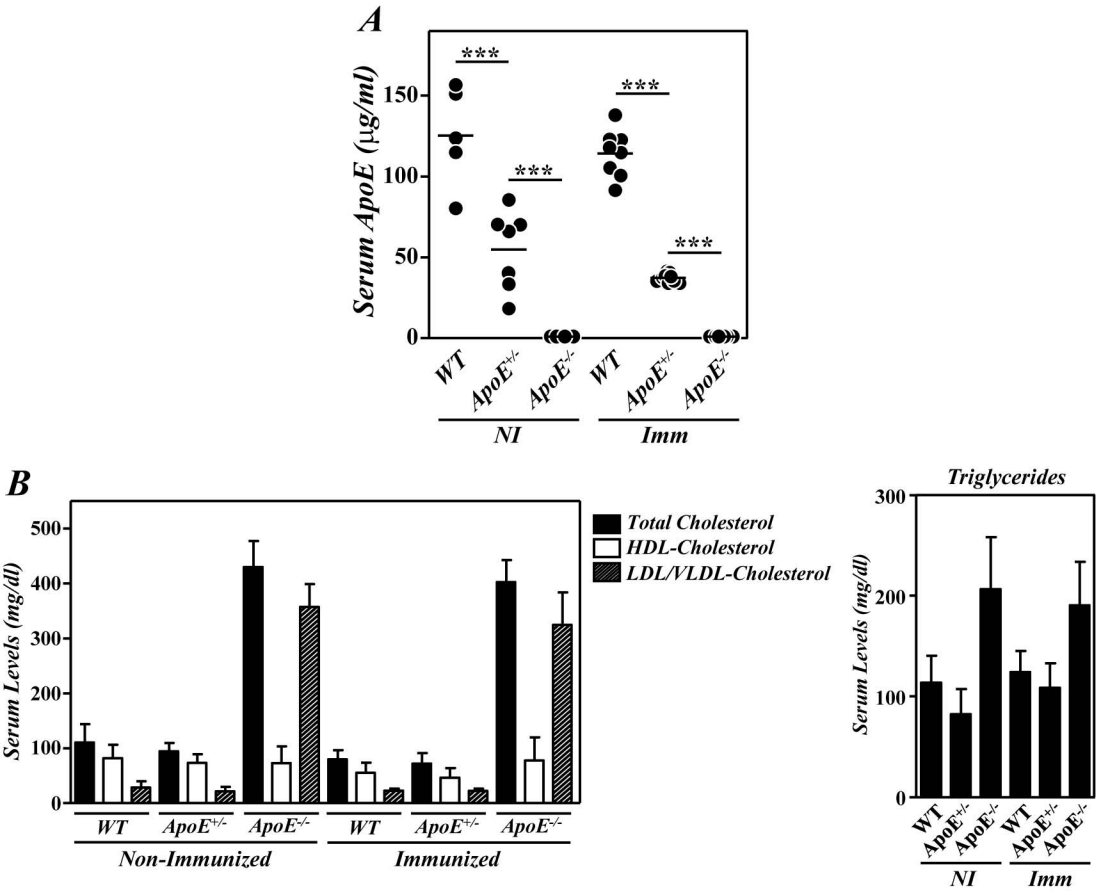

Figure 1

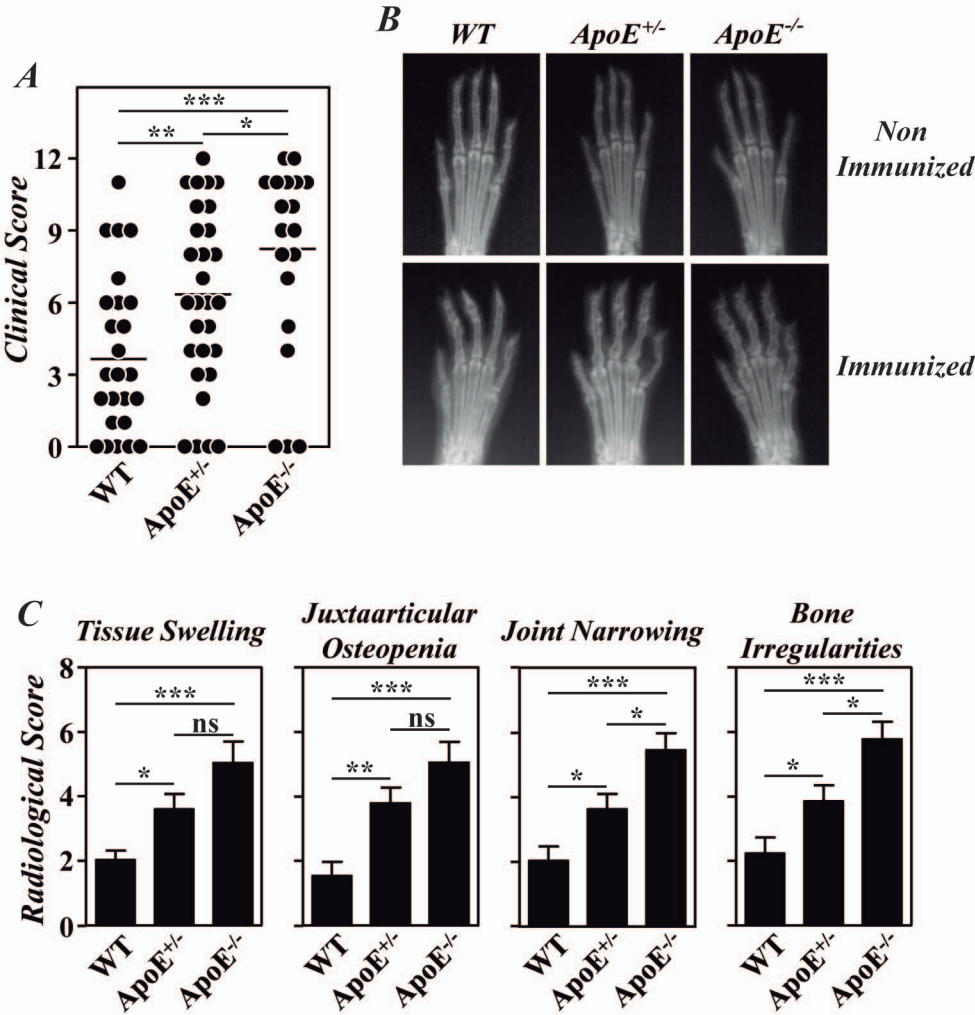

Figure 2

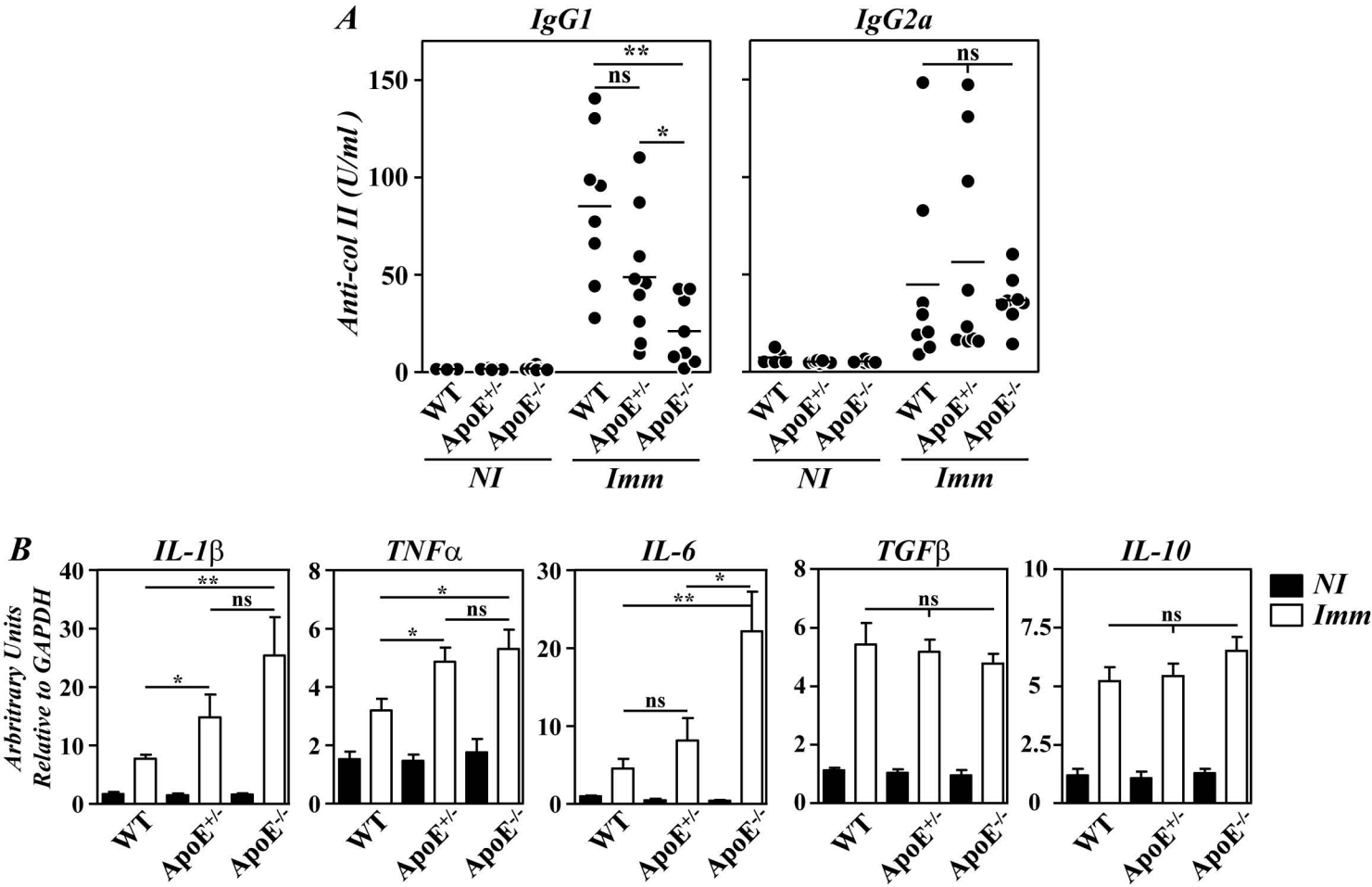

Figure 3

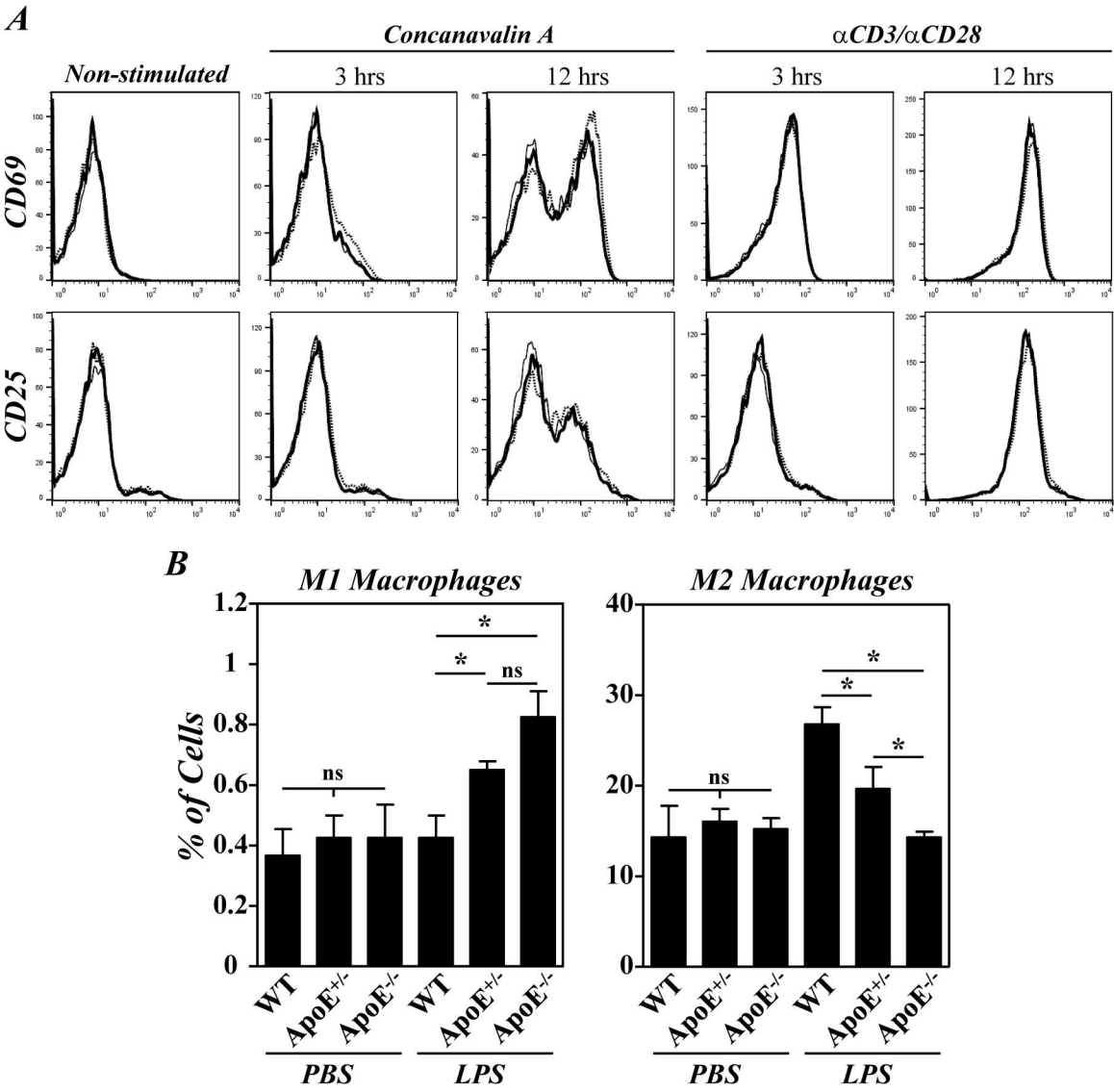

Figure 4

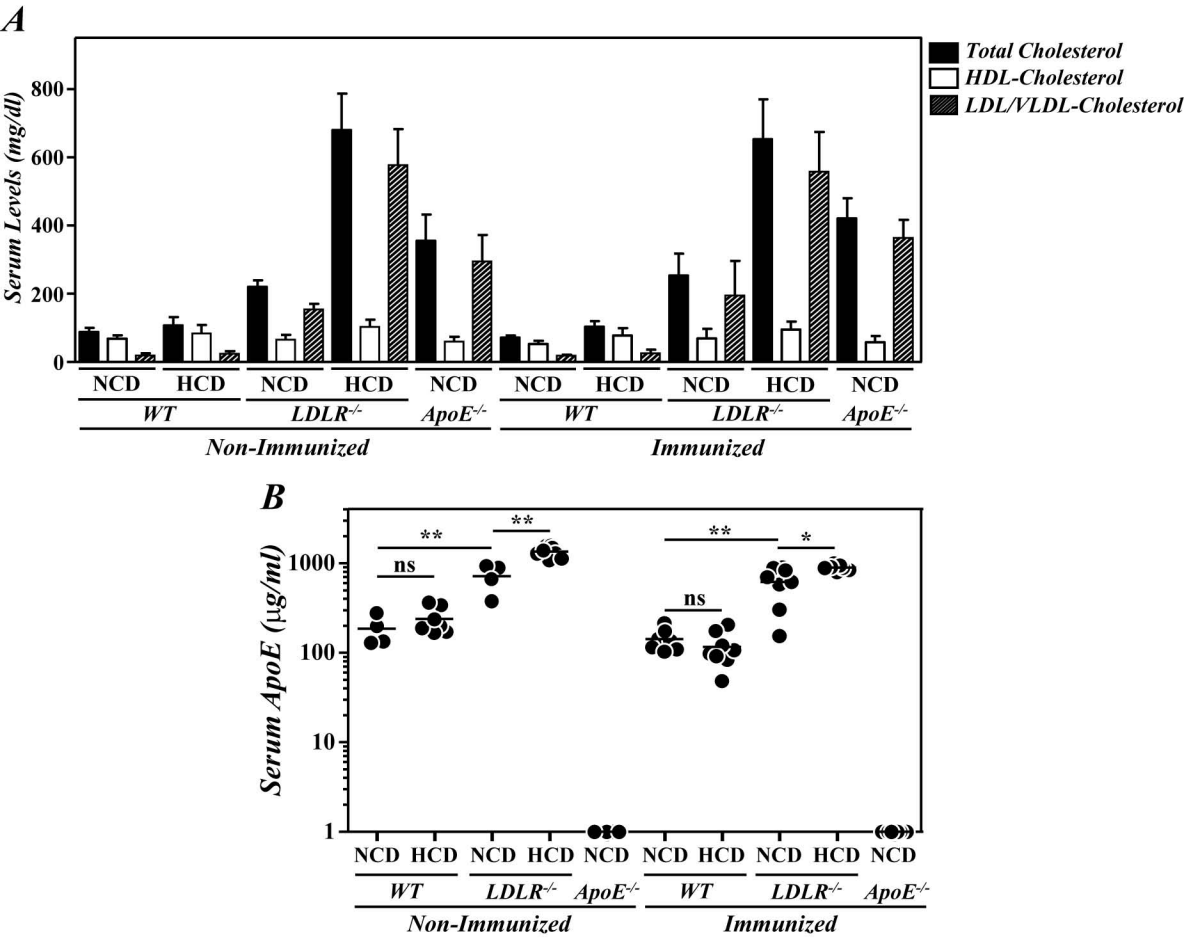

Figure 5

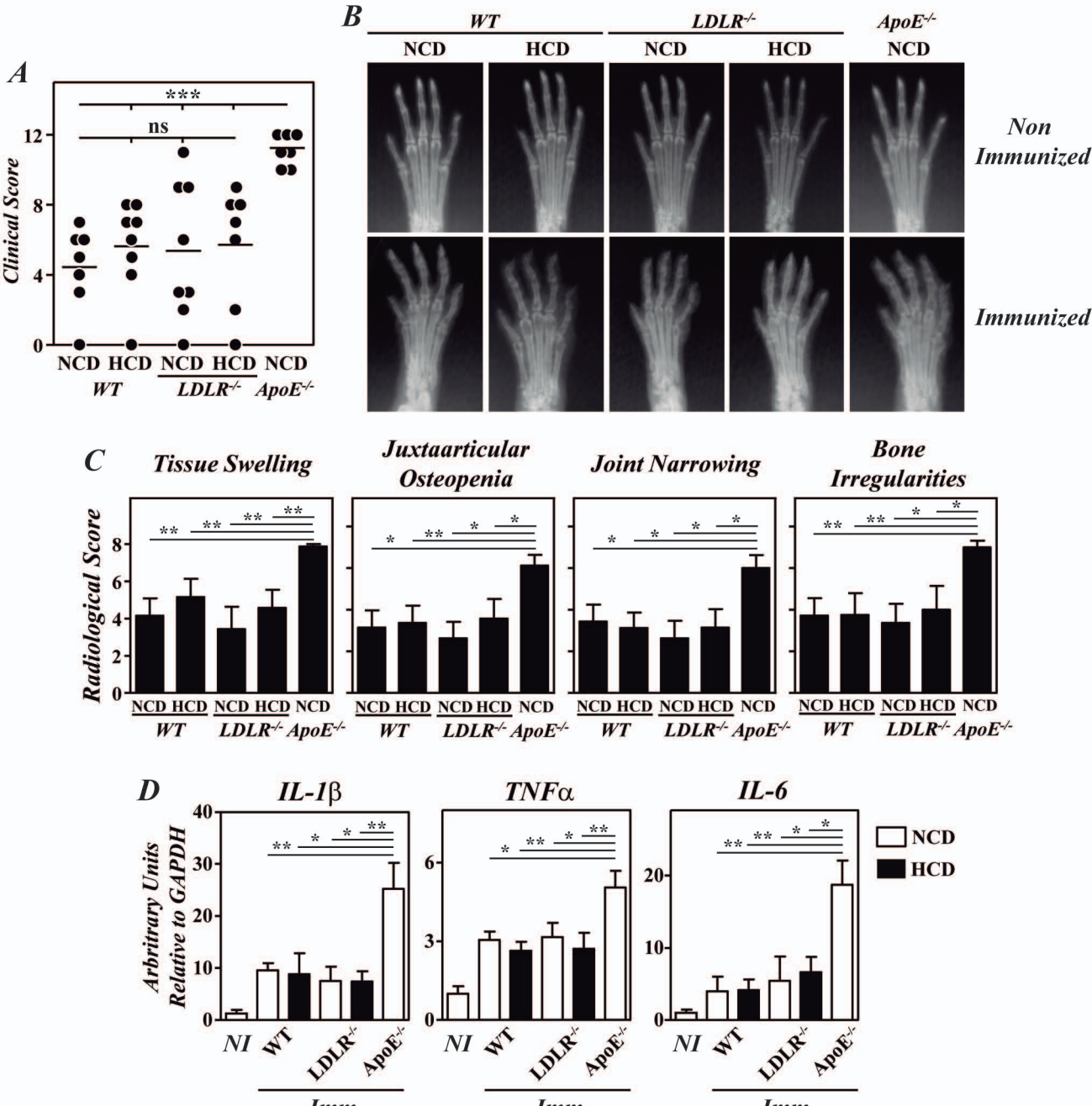

Figure 6